Report

Cell Reports

A MicroRNA-Based Gene-Targeting Tool for Virally Labeling Interneurons in the Rodent Cortex

Graphical Abstract

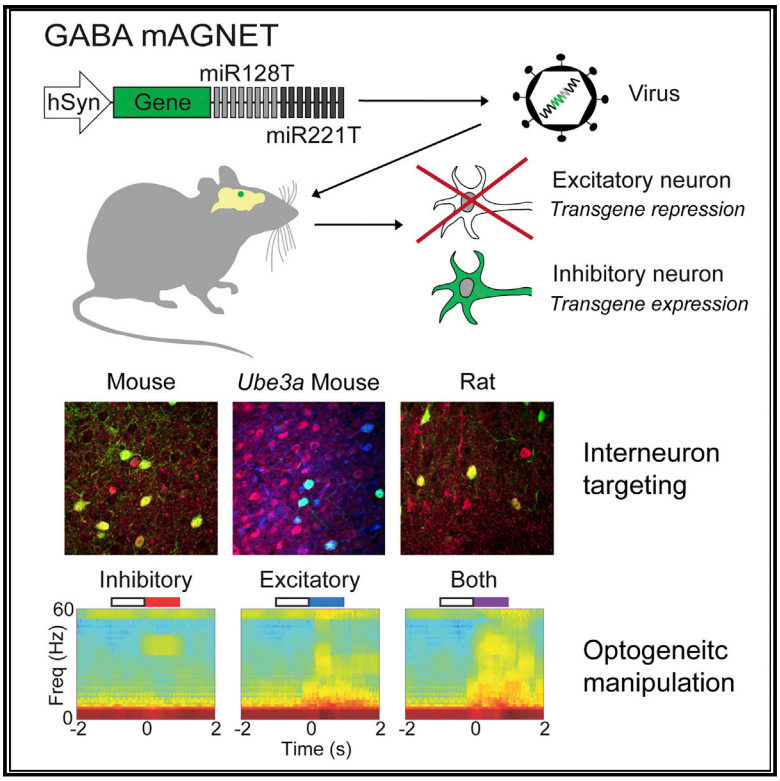

Highlights

- Developed GABA mAGNET, a miRNA-based viral gene delivery tool for interneurons
- GABA mAGNET achieves >95% cortical interneuron targeting in mice
- GABA mAGNET works in a mouse autism model and exhibits some functionality in rats
- GABA mAGNET enables viral-mediated optogenetic manipulation of two neuron subtypes

Authors

Marianna K. Keaveney, Hua-an Tseng, Tina L. Ta, Howard J. Gritton, Heng-Ye Man, Xue Han

Correspondence

xuehan@bu.edu

In Brief

Viral targeting of neuron subtypes is desirable for neuroscience research. Keaveney et al. developed a microRNA-based viral tool for labeling cortical interneurons. They demonstrate its utility via neuron subtype labeling in a murine disease model and in rats and through dual-color optogenetic control of two neuron types.

Keaveney et al., 2018, Cell Reports *24*, 294–303
July 10, 2018
https://doi.org/10.1016/j.celrep.2018.06.049

CellPress

OPEN ACCESS
CellPress

Cell Reports
Report

A MicroRNA-Based Gene-Targeting Tool for Virally Labeling Interneurons in the Rodent Cortex

Marianna K. Keaveney,[1] Hua-an Tseng,[1] Tina L. Ta,[1] Howard J. Gritton,[1] Heng-Ye Man,[2] and Xue Han[1,3,*]
[1]Department of Biomedical Engineering, Boston University, Boston, MA 02215, USA
[2]Department of Biology, Boston University, Boston, MA 02215, USA
[3]Lead Contact
*Correspondence: xuehan@bu.edu
https://doi.org/10.1016/j.celrep.2018.06.049

SUMMARY

More specific and broadly applicable viral gene-targeting tools for labeling neuron subtypes are needed to advance neuroscience research, especially in rodent transgenic disease models and genetically intractable species. Here, we develop a viral vector that restricts transgene expression to GABAergic interneurons in the rodent neocortex by exploiting endogenous microRNA regulation. Our interneuron-targeting, microRNA-guided neuron tag, "GABA mAGNET," achieves >95% interneuron selective labeling in the mouse cortex, including in a murine model of autism and also some preferential labeling of interneurons in the rat brain. We demonstrate an application of our GABA mAGNET by performing simultaneous, *in vivo* optogenetic control of two distinct neuron subtypes. This interneuron labeling tool highlights the potential of microRNA-based viral gene targeting to specific neuron subtypes.

INTRODUCTION

A wide variety of genetically encoded sensors and actuators are revolutionizing neuroscience research. Over the years, whole-animal transgenic techniques have been successful in mice for targeted gene expression in specific neuron subtypes (Tamamaki et al., 2003; Taniguchi et al., 2011). For other experimental mammalian models and for human gene therapy, transgenic strategies remain limited or impractical, and viral gene delivery remains an effective, time-efficient strategy to transduce post-mitotic neurons (Blessing and Déglon, 2016). Additionally, when used in transgenic lines, viral gene delivery further expands the capacity to express different molecules in neuron subtypes. A major challenge in developing viral gene delivery tools is the limited DNA packaging capacity of the most commonly used viral vectors, lentivirus (LV) and adeno-associated virus (AAV) (Gray et al., 2010; Blessing and Déglon, 2016). Thus, the use of cell-type-specific promoter and enhancer elements for viral gene delivery has been mainly limited to a few neuron types, as the large size and the complexity of these natural elements often leads to complications with viral packaging or transgene expression (Dittgen et al., 2004; Nathanson, et al., 2009a).

We recently explored the use of microRNA (miRNA) regulation, a gene regulation mechanism orthogonal to promoter elements, to restrict gene expression to specific subsets of neurons and illustrated the synthetic biology design principles involved (Sayeg et al., 2015). This strategy is uniquely suited for virally delivered genetic classifiers because miRNA recognition sites are small (~22 nt) and can be easily packaged in viral vectors. Additionally, miRNA targeting is highly engineerable: several miRNAs each with multiple recognition site repeats can be combined to regulate the expression of a single gene. Finally, miRNAs are particularly enriched in the mammalian brain compared to other organs (Nelson et al., 2008), making them highly suitable for neuroscience applications.

Inhibitory neurons (~20% of cortical neurons) play an essential role in regulating neural network activity, and their dysfunction has been implicated in various brain disorders (Marín, 2012). For example, imbalanced excitation and inhibition have been linked to autism spectrum disorders (ASD) (Nelson and Valakh, 2015). While transgenic mouse lines have revolutionized our ability to target specific interneuron types (Taniguchi et al., 2011), it remains difficult to cross-breed transgenic driver lines with transgenic disease models. Virally targeting interneurons has been demonstrated using shortened or non-mammalian promoters (Nathanson et al., 2009a; Delzor et al., 2012) or short cell-type-specific enhancer elements (Lee et al., 2014; Vogt et al., 2014; Dimidschstein et al., 2016). miRNA regulation is orthogonal to promoter and enhancer regulatory elements and represents an additional strategy to achieve interneuron targeting from viral vectors.

In this study, we developed a miRNA-guided neuron tag ("mAGNET") to restrict transgene expression to cortical inhibitory (GABA+) neurons in the mouse neocortex (GABA mAGNET). GABA mAGNET achieves 98% cortical interneuron targeting selectivity in mice. To illustrate the utility of this tool, we demonstrated neuron subtype labeling in a *Ube3a* (2xTg) transgenic mouse model of autism, established some cross-species functionality in the rat cortex and hippocampus, and performed dual-color optogenetic manipulation of distinct neuron subtypes in non-transgenic mice. This work highlights the promise of miRNA-based gene targeting for basic brain research and translational applications.

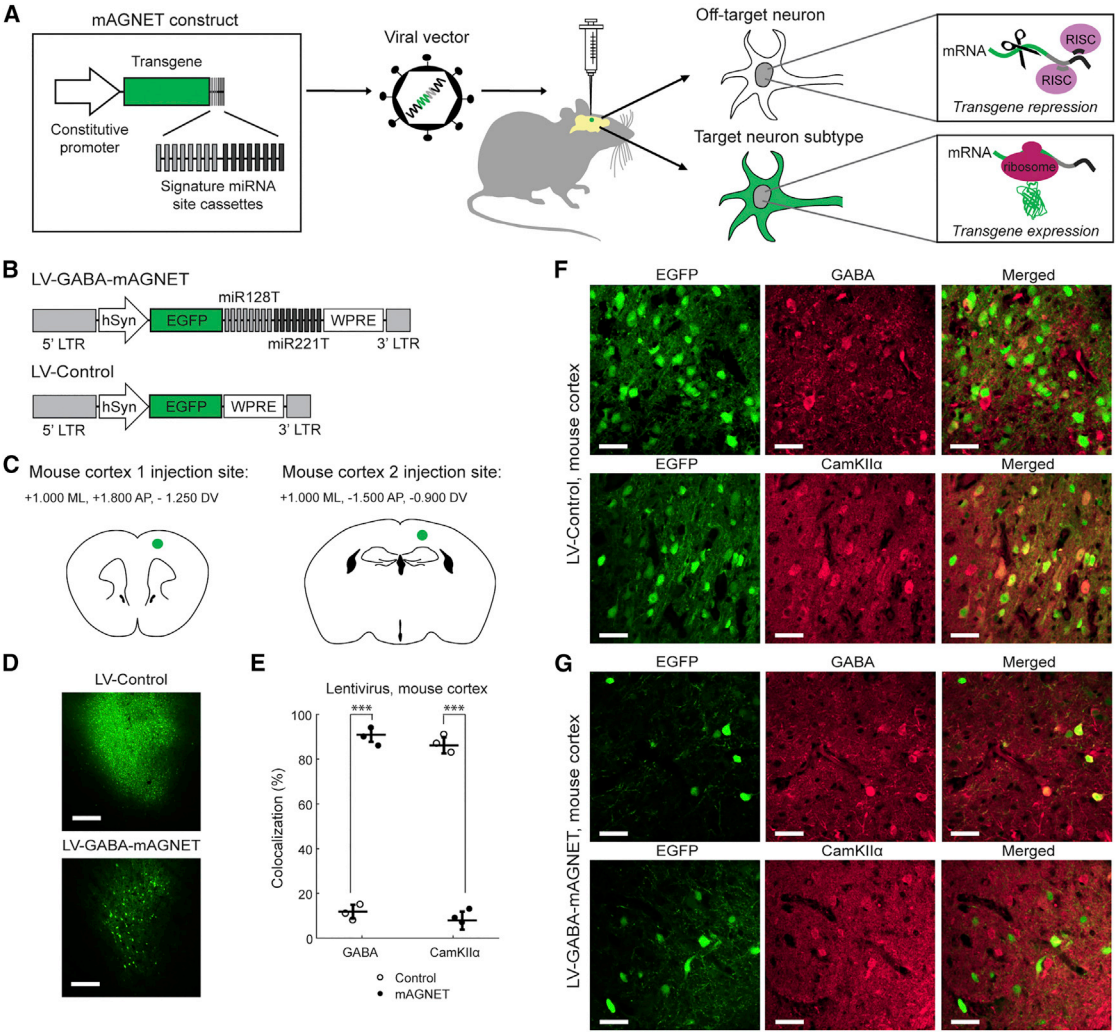

Figure 1. mAGNET Gene-Targeting Strategy and LV-GABA-mAGNET Targeting in the Mouse Cortex

(A) Schematic of viral, microRNA-guided neuron tag (mAGNET) gene-targeting strategy.

(B) LV-GABA-mAGNET and LV-Control lentiviral vector designs; LTR = long terminal repeat, hSyn = human synapsin promoter, EGFP = enhanced green fluorescent protein, and WPRE = woodchuck hepatitis virus post-regulatory element. miR128T/miR221T refer to cassettes of eight respective miRNA target sites – note that these sites are not shown to scale—they are enlarged for visualization purposes.

(C) Schematics of stereotaxic virus injection sites in mouse cortex.

(D) Confocal microscopy images showing comparison of lentivirus transduction in WT mouse cortex (cortex 1 injection site). Scale bars, 250 μm.

(E) Colocalization of EGFP+ cells with inhibitory (GABA) and excitatory (CamKIIα) cell markers in the WT mouse cortex (n = 3 mice each). Scatterplot shows individual animals (circles) and mean (horizontal bar) ± SD. ***$p < 0.005$, Pearson's chi-square test.

(F and G) Representative confocal images of EGFP+ cortical cells transduced with LV-Control (F) or LV-GABA-mAGNET (G), immunofluorescence of inhibitory (GABA) and excitatory (CamKIIα) cell markers, and colocalization. Scale bars, 35 μm.

See also Figure S1 and Tables S1 and S2.

RESULTS

hSyn-Driven Lentiviral GABA mAGNET Targets Interneurons with 91% Selectivity in Mouse Cortex

Figure 1A illustrates the mAGNET gene-targeting strategy, where we can utilize a constitutive promoter to drive gene expression non-specifically and encode cellular specificity by including "signature" miRNA target or recognition sites (miRT) within the 3′ untranslated region of the gene. Because miRNA regulation is an inhibitory mode of gene expression control, signature miRNAs are chosen based on their higher expression levels in off-target cells compared to the on-target cells (Sayeg et al., 2015). The designed mAGNET vector, when packaged as a virus and injected at a specific location in the brain, leads to the production of transcripts in all infected cells. However, signature miRNAs in off-target cells inhibit gene expression by hybridizing to their complementary target sites within the mAGNET transcript. Conversely, the low level of signature

miRNAs in the on-target cell type permits the mAGNET transcripts to be translated and expressed.

To label GABA+ interneurons in the mouse cortex, we selected two signature miRNAs with both high expression levels in off-target excitatory neurons and the highest ratios of expression from excitatory to inhibitory neurons: mir-128 and mir-221 (He et al., 2012). Mir-128 is one of the most highly expressed miRNAs in the mammalian brain (Lagos-Quintana et al., 2002) and is known to be an essential regulator of genes involved in neuronal excitability (Tan et al., 2013). Mir-221 is known to play a role in tumor angiogenesis (Santhekadur et al., 2012), although its function in brain tissue is unknown. Our previous work demonstrated that eight sites for mir-128 and mir-221 each resulted in some restriction of gene expression to interneurons (Sayeg et al., 2015).

To generate a highly specific interneuron mAGNET, we explored orthogonal elements of the gene delivery system, starting with the constitutive promoter that drives mAGNET expression. Our previous designs utilized a strong EF1α promoter (Sayeg et al., 2015). However, we reasoned that this strong promoter that drives transcription at a high rate, may hinder effective regulation by endogenous neural microRNAs in off-target cells. We therefore employed the pan-neuronal human synapsin 1 promoter (hSyn, 480 bp) (Figure 1B), which mediates neuron-specific, long-term transgene expression from viral vectors (Kügler et al., 2003). We packaged the hSyn-driven LV-GABA-mAGNET and LV-Control vectors as lentiviruses pseudotyped with vesicular stomatitis virus glycoprotein (VSVG) envelope protein and injected each at two locations in the adult, wild-type (WT) mouse cortex (n = 3 mice per virus) (Figure 1C). Fluorescence image analysis at two weeks post-injection revealed that virally transduced EGFP+ cells in the mAGNET-infected mice were more sparsely distributed compared to the control (Figure 1D). Furthermore, individual EGFP+ neurons were clearly visible without immunostaining and exhibited no observable difference in fluorescence intensity between the LV-GABA-mAGNET and LV-Control or compared to previous EF1α-driven lentiviruses (Sayeg et al., 2015). These results suggest that LV-GABA-mAGNET virus infected cells within a comparable volume to the LV-Control virus and the sparse distribution of EGFP+ cells is consistent with the distribution of inhibitory neurons in the mammalian neocortex.

Examining brain slices, we assessed interneuron targeting selectivity—defined as the percentage of EGFP+ neurons that colocalize with a GABA immunofluorescence marker for cortical inhibitory neurons. We also independently quantified EGFP co-localization with a CamKIIα immunofluorescence marker for cortical excitatory neurons (off-target cells) as a complimentary measure. The LV-Control vector (with no miRNA sites) exhibited ~12% GABA targeting selectivity (and ~86% colocalization with CamKIIα immunofluorescence) (Figures 1E and 1F; Table S1), consistent with previous observations of a slight tropism toward excitatory neurons with VSVG-pseudotyped lentivirus (Nathanson et al., 2009b; Sayeg et al., 2015). In contrast, the LV-GABA-mAGNET predominantly labeled interneurons, exhibiting 91 ± 3% target selectivity (Figures 1E and 1G; Table S1). Targeting was consistent at both cortical injection locations (Figure S1A).

AAV Packaging Improves GABA mAGNET Targeting Selectivity to 98%

We next explored whether adeno-associated virus (AAV) packaging would further improve interneuron targeting selectivity, given the excitatory-neuron tropism of VSVG-pseudotyped lentivirus (Nathanson et al., 2009b; Sayeg et al., 2015). AAV is commonly used in biomedical research and in human gene therapy (Xu et al., 2001; Nathanson, et al., 2009b; Aschauer, et al., 2013; Maguire et al., 2014; Watakabe et al., 2015). Recently, a systematic comparison of AAV serotypes 1, 2, 5, 6, 8, and 9 in the mouse brain demonstrated that AAV serotype 9 is most efficient for transducing cortical neurons, with slight tropism toward cortical inhibitory neurons (Aschauer et al., 2013). We thus packaged the hSyn-driven GABA mAGNET as AAV2.9 (using AAV-2 genomic backbone pseudotyped with AAV-9 capsid protein) to further improve interneuron targeting (Figure 2A). Because AAVs have a small packaging capacity (~5 kb) compared to lentivirus (~10 kb), the compact size of the miRNA recognition sites, as well as, the short hSyn promoter were especially important for efficient packaging in AAVs.

We injected AAVs at the cortex 1 injection site (Figure 1C) in adult, WT mice (n = 3 mice per virus), since we previously observed no differences in interneuron targeting across cortical locations (Figure S1). We processed the brain tissue at three weeks post-injection (Figure 2B) and found that the AAVs (Figure 2B) infected a broader region than lentivirus (Figure 1D), consistent with the ability to package AAVs at higher titers (AAV titer: ~2E12 vg/mL, ~0.5 μL injected versus LV titer: ~1E9 infectious particles/mL, ~1 μL injected). Of the AAV-Control transduced EGFP+ cells, 23 ± 2% are GABA+ cells (76 ± 4% are CamKIIα+) (Figures 2C and 2D; Table S1), consistent with the general observation that AAV2.9 exhibits a slight transduction bias toward cortical inhibitory neurons. With this transduction bias, AAV-GABA-mAGNET exhibits 98 ± 2% targeting selectivity for cortical interneurons (Figures 2C and 2E; Table S1), achieving the cell-type targeting standards set by transgenic animals (Tamamaki et al., 2003; Taniguchi et al., 2011).

To determine whether AAV-GABA-mAGNET preferentially labeled a particular interneuron subtype, we performed immunohistochemistry with non-overlapping interneuron subtype markers, parvalbumin (PV), and calretinin (CR). We found that EGFP+ cells expressed these markers in the proportions corresponding to their expected distributions in mouse cortex (Xu et al., 2006; Gonchar et al., 2008; Rudy et al., 2011; Tremblay et al., 2016) (Figure S2). Thus, AAV-GABA-mAGNET is highly specific for cortical interneurons without a labeling bias between interneuron subtypes.

AAV GABA mAGNET Targets Cortical Interneurons with 95% Selectivity in a Transgenic Autism Mouse Model

Viral vector-mediated gene targeting is especially useful in transgenic disease models because it offers the opportunity of cell-type-specific investigation without the need of cross-breeding with cell-type-specific transgenic drive lines. Accordingly, we demonstrated the utility of our AAV-GABA-mAGNET in a mouse autism model with overexpression of the autism risk gene *Ube3a* (Smith et al., 2011). To examine the targeting selectivity of GABA mAGNET in *Ube3a* (2XTg) mice, we

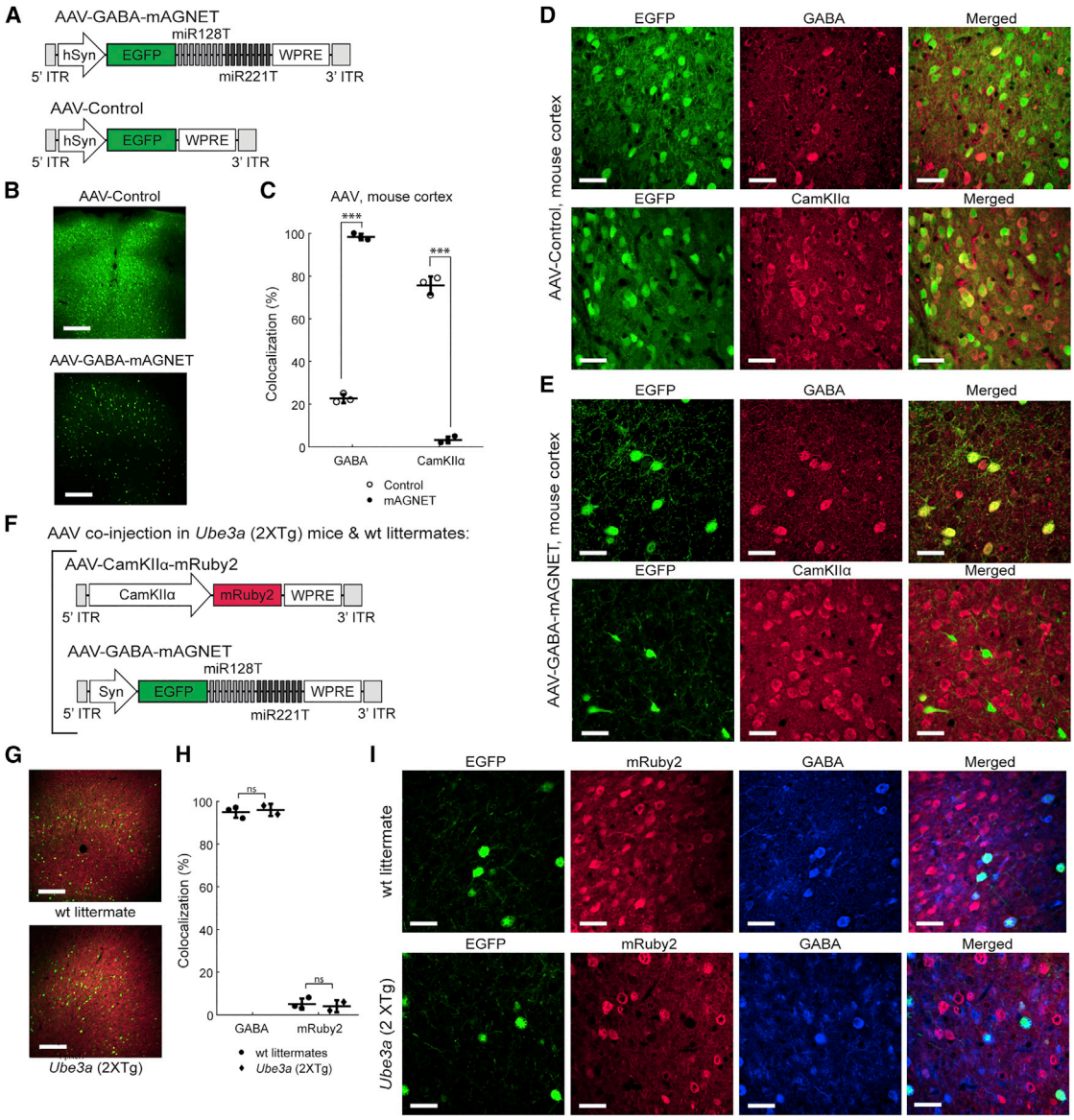

Figure 2. Selective Interneuron Labeling with rAAV2.9 Packaged GABA mAGNET in the Mouse Cortex

(A) AAV-GABA-mAGNET and AAV-Control vector designs.

(B) Confocal microscopy images showing comparison of AAV transduction in C57bL/6 WT mouse cortex (cortex 1 site). Scale bars, 250 μm.

(C) Colocalization of EGFP+ cells with inhibitory and excitatory marker immune stains in the C57bL/6 WT mouse cortex (n = 3 mice each). Scatterplot shows individual animals (circles) and mean (horizontal bar) ± SD. ***p < 0.005, Pearson's chi-square test (see Experimental Procedures).

(D–E) Representative confocal images of EGFP+ cortical cells transduced with AAV-Control (D) or AAV-GABA-mAGNET(E), immunofluorescence of inhibitory (GABA) and excitatory (CamKIIα) cell markers, and colocalization. Scale bars, 35 μm.

(F) Co-injected AAV-CamKIIα-mRuby2 and AAV-GABA-mAGNET viral vector designs.

(G) Confocal microscopy images showing cells transduced by AAV-CamKIIα-mRuby2 (red) and AAV-GABA-mAGNET (green) in the cortex (cortex 1 site) of a *Ube3a* (2xTg) autism model mouse versus FVP WT littermate. Scale bars, 250 μm.

(H) Colocalization of EGFP+ cells (transduced by AAV-GABA-mAGNET) with GABA immunofluorescence or mRuby2 (transduced by AAV-CamKIIα-mRuby2) in *Ube3a* (2xTg) mice (n = 2) and WT littermates (n = 3). Scatterplot shows individual animals (circles) and mean (horizontal bar) ± SD ns = no significance, Pearson's chi-square test.

(I) Representative confocal images of EGFP+ cortical cells transduced with AAV-GABA-mAGNET, mRuby2 fluorescence from cortical cells transduced with AAV CamKIIα mRuby2, immunofluorescence of an inhibitory (GABA) cell marker, and colocalization from a *Ube3a* (2xTg) mouse (bottom) and WT littermate (top). Scale bars, 35 μm.

See also Figures S1and S2 and Tables S1 and S2.

co-injected AAV-GABA-mAGNET with AAV-CamKIIα-mRuby2 (Figure 2F), a virus that uses a shortened CamKIIα promoter (Dittgen et al., 2004) to drive expression of the red fluorescent mRuby2 reporter in cortical excitatory neurons. These AAVs were co-injected at the cortex 1 location (Figure 1C) in adult *Ube3a* (2xTg) mice and WT FVP littermate controls. At three weeks post-injection, we found that the total number of transduced EGFP+ neurons was similar between the *Ube3a* (2XTg) mice and WT littermates (Figure 2G). Of the transduced EGFP+ cells, 96 ± 2% are GABA+ in the *Ube3a* (2xTg) mice and similarly, 95 ± 3% in the WT littermates (Figures 2H and 2I; Table S1). Together, these results suggest that signature miRNA expression is similar between the WT and autistic transgenic mice and between the FVP and C57b/L6 genetic background. Furthermore, we achieved viral-mediated labeling of two neuron subtypes (inhibitory and excitatory neurons) (Figures 2G–2I), illustrating how our GABA mAGNET will allow further characterization of disease mechanisms and therapeutic strategies in disease models.

Interneuron Targeting with GABA mAGNET in the Rat Brain

Rats are another preferred animal model but with limited gene-targeting tools available. Because there is a high degree of miRNA sequence conservation across mammals and especially between rodents (Bak et al., 2008; Minami et al., 2014), we hypothesized that mouse-derived GABA mAGNETs might achieve some interneuron selectivity in the rat brain. We injected GABA mAGNET and control viruses in adult, WT rats (n = 3 per virus) at two cortical sites equivalent to the coordinates in the mice (see Supplemental Experimental Procedures). We again observed that labeled neurons were much sparser in the mAGNET animals compared to the controls (Figures 3A and 3E). LV-Control and AAV-Control virus primarily labeled excitatory neurons with limited interneuron target selectivity (16% for LV-Control [Figures 3B and 3C; Table S1] and 21% for AAV-Control [Figures 3G and 3F; Table S1]). The LV-GABA-mAGNET achieved 74 ± 3% interneuron targeting selectivity (Figures 3B, 3D, and S1B; Table S1), and AAV-GABA-mAGNET exhibited a higher interneuron targeting selectivity of 82 ± 2% (Figures 3F and 3H; Table S1). When tested in the rat hippocampus (Figure S3A), AAV-GABA-mAGNET achieved 80 ± 5% interneuron targeting selectivity (Figures S3C and S3E; Table S1). Together, these results demonstrate that miRNA-based gene-targeting exhibits some cross-species and cross-brain region functionality, and further miRNA profile data in rats could facilitate the design of mAGNETs with improved targeting selectivity.

GABA mAGNET Enables Dual-Color Optogenetic Manipulation of Two Neuron Types

To demonstrate an application of our optimized GABA mAGNET, we performed dual-color optogenetic manipulation of two neuron types in the WT mouse cortex using Jaws and ChR2—rhodopsins that have minimal spectral overlap (Chuong et al., 2014; Klapoetke et al., 2014). We co-injected two AAVs: AAV-Jaws-GABA-mAGNET, which mediates Jaws-mRuby2 expression to inhibitory neurons and allows them to be silenced with red light, and AAV-CamKIIα-ChR2, which mediates ChR2-EGFP expression in CamKIIα+ excitatory neurons and allows these cells to be activated with blue light (Figure 4A). Immunostaining results verified that interneuron targeting selectivity with the AAV-Jaws-GABA-mAGNET remained high (95 ± 3%).

Four weeks after injection, we recorded local field potentials (LFPs) while silencing inhibitory neurons (expressing Jaws) with red light or activating excitatory neurons (expressing ChR2) with blue light, or both simultaneously. We applied two illumination patterns: a 1 s long pulse train at 40 Hz or a single 200-ms-long pulse. In mAGNET mice, 40 Hz illumination with either the red or the blue light alone was sufficient to induce oscillations centered at 40Hz and concurrent illumination with both blue and red light induced stronger oscillations (Figure 4C). At a population level, across all animals, we found that silencing the inhibitory neurons with 40 Hz red light led to a significant increase in LFP oscillation power, centered at 40 Hz (n = 6 mice) (Figures 4Dii and 4E, left [$p < 0.05$, Wilcoxon rank-sum test]). Activating the excitatory neurons with 40 Hz blue laser illumination, either alone or simultaneously with silencing the inhibitory neurons, produced stronger oscillations (Figures 4Dii and 4E, middle and right [$p < 0.05$]). These results demonstrate that both Jaws and ChR2 were expressed at functional levels in separate cell types and can be effectively optogenetically controlled; therefore, miRNA regulatory cassettes did not hinder rhodopsin expression in the on-target cells. The same 40 Hz laser illuminations produced no change in sham mice (no virus injection) as expected (n = 5) (Figures 4Ci and 4Di).

With 200 ms pulse illumination, red or blue light alone only elicited small changes in the LFPs, but simultaneous illumination with red and blue light consistently enhanced power at higher frequencies (Figure 4F). At a population level, across all animals, we found that silencing the inhibitory neurons or activating the excitatory neurons with a 200 ms pulse of red light produced little effect (n = 6) (Figure 4Gii, left and middle). Simultaneous inhibitory silencing and excitatory activation induced increases in LFP power over a wide frequency range (Figure 4Gii, right). At gamma frequencies, neither inhibitory silencing nor excitatory activation alone was sufficient to produce significant changes, but simultaneous silencing of inhibitory neurons and activation of excitatory neurons led to significantly stronger gamma oscillations ($p < 0.05$, Wilcoxon rank-sum test) (Figure 4H). This summation phenomenon confirms successful optogenetic control of both neuron types. 200 ms laser illuminations in sham mice (without virus injection) produced no effects (Figures 4Fi and 4Gi). Together, these results suggest that activation of excitatory neurons and inhibition of inhibitory neurons have an additive effect on network dynamics, when each perturbation produces small changes (Figure 4H [with 200ms long light illumination]). However, when excitatory neurons were driven strongly by ChR2, silencing of inhibitory neurons failed to further enhance oscillation power at gamma frequencies (Figure 4E [1 s light illumination at 40 Hz]).

DISCUSSION

In this study, we have developed GABA mAGNET: a miRNA-based, viral gene delivery tool that restricts transgene expression to cortical inhibitory neurons in mice. Integrating synthetic

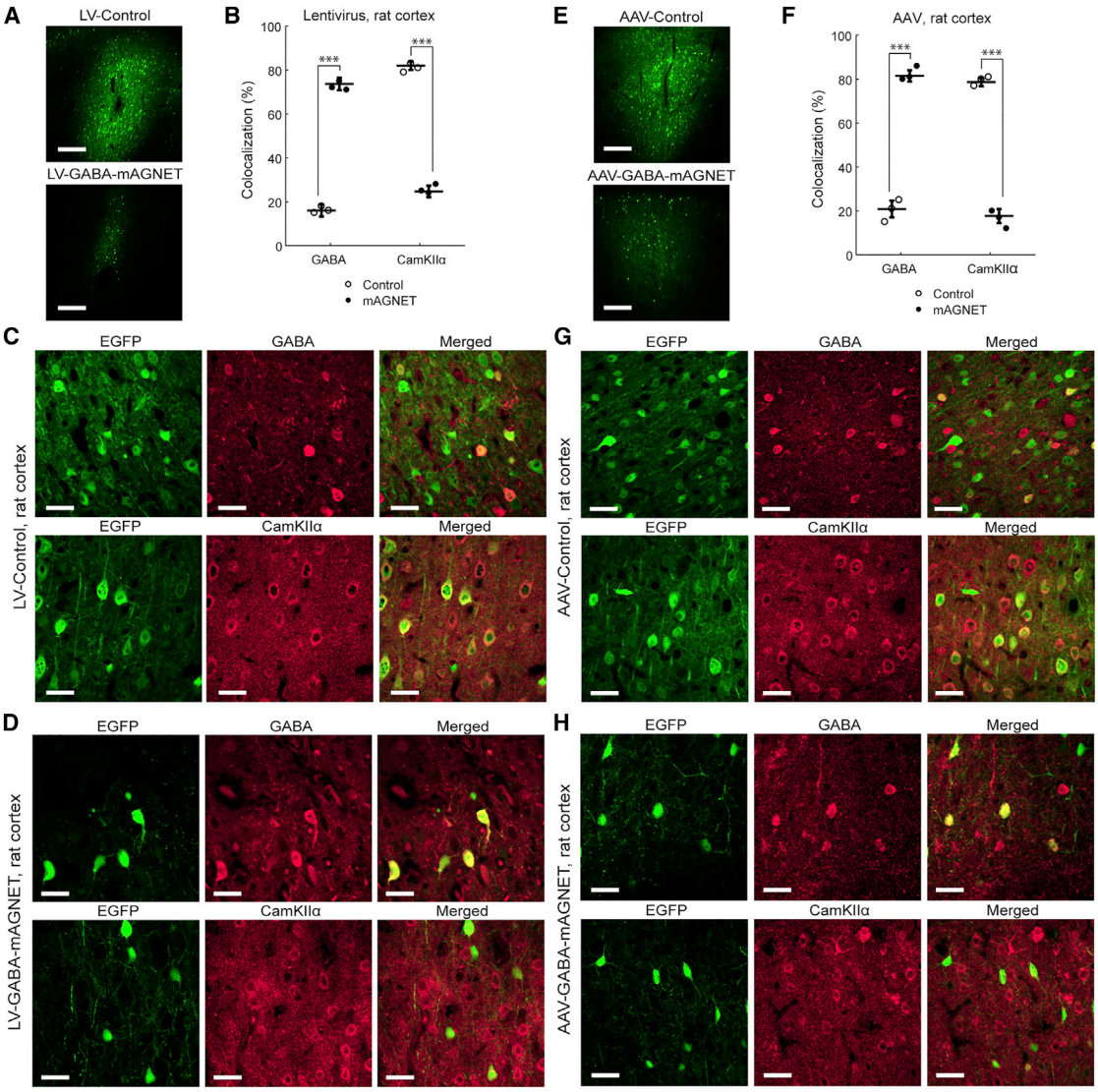

Figure 3. Interneuron Targeting with GABA mAGNETs in the Rat Cortex

(A) Confocal microscopy images showing comparison of lentivirus transduction in rat cortex (cortex 1 site). Scale bars, 250 μm.

(B) Colocalization of EGFP+ cells with inhibitory and excitatory marker immune stains in rat cortex (n = 3 rats each). Scatterplot shows individual animals (circles) and mean (horizontal bar) ± SD. ***p < 0.005, Pearson's chi-square test.

(C) Representative confocal images of EGFP+ cortical cells transduced with LV-Control, immunofluorescence of inhibitory (GABA) and excitatory (CamKIIα) cell markers, and colocalization. Scale bars, 35 μm.

(D) Same as (C), for cells transduced with LV-GABA-mAGNET.

(E–H) Same as (A–D), for AAV-Control and AAV-GABA-mAGNET.

See also Figures S1 and S3 and Tables S1 and S2.

biology principles on designing signature miRNA binding site cassettes and promoter and viral packaging designs, we report a GABA mAGNET with >95% targeting selectivity toward cortical inhibitory neurons, comparable to that achieved with whole-animal transgenic techniques (Tamamaki et al., 2003; Taniguchi et al., 2011). This interneuron targeting tool remains effective at labeling cortical interneurons in *Ube3a* 2X Tg transgenic murine model of autism, where transgenic cell-type targeting is difficult. We also demonstrate that GABA mAGNET exhibits ≥80% interneuron specificity in the rat cortex and hippocampus. Finally, to illustrate the possible application of the GABA mAGNET targeting tool, we used it to perform a dual-color optogenetic manipulation of distinct neuron subtypes in non-transgenic mice, highlighting the promise of miRNA-based gene targeting in basic brain research and translational applications.

The mAGNET strategy offers several unique advantages for gene delivery in the brain. First, miRNAs are particularly enriched in the mammalian brain (Nelson et al., 2008), are important in

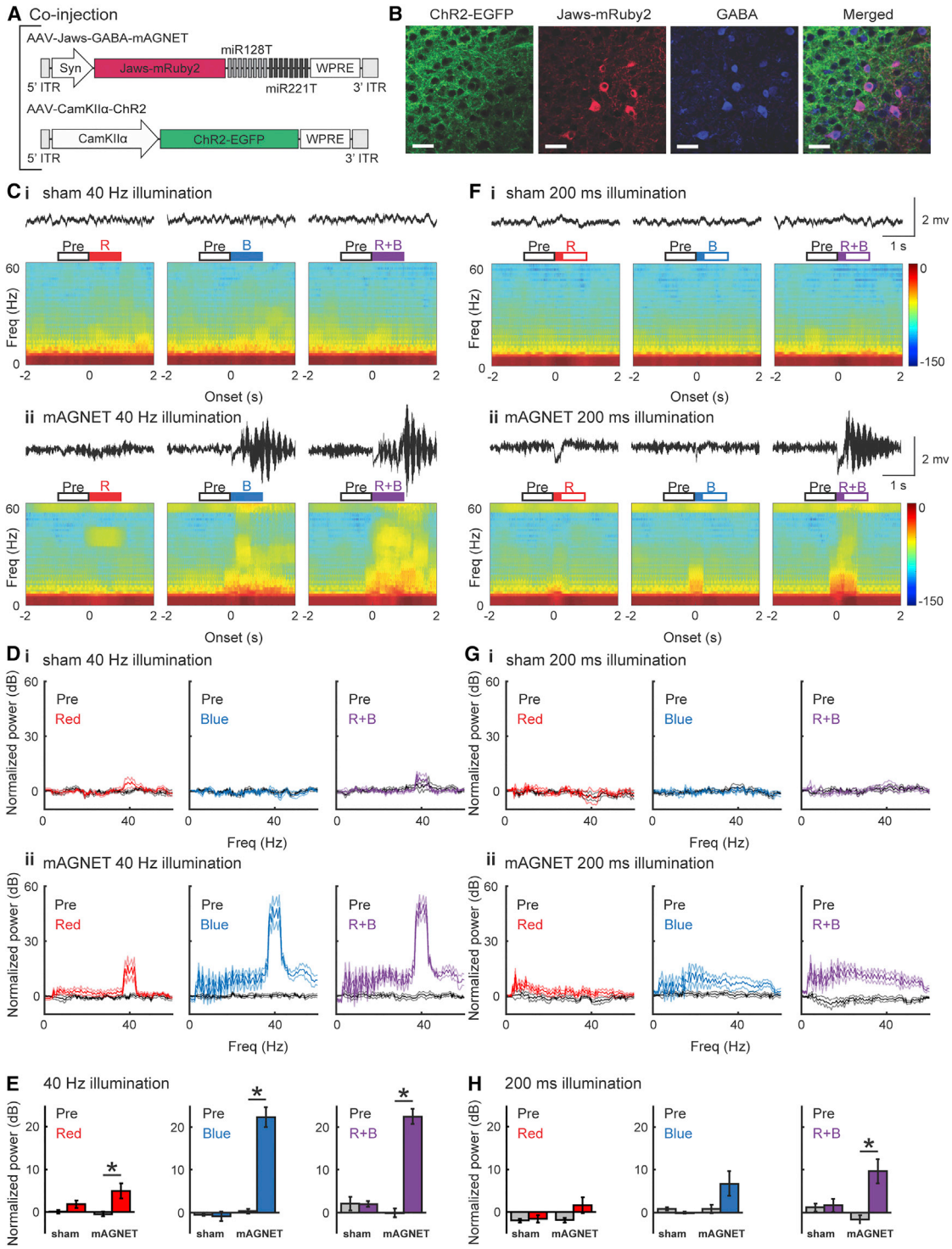

Figure 4. Simultaneous Optogenetic Manipulation of Two Neuron Subtypes *In Vivo* with AAV-GABA-mAGNET

(A) AAV vector designs to selectively express Jaws-mRuby2 in cortical inhibitory neurons for silencing (AAV-Jaws-GABA-mAGNET), and ChR2-EGFP in cortical excitatory neurons for activation (AAV-CamKIIα-ChR2).

(B) Representative confocal images of CHR2-EGFP expression, Jaws-mRuby2 expression, GABA immunostaining, and colocalization. Scale bars, 35 μm.

(C) Examples of local field potential (LFP) recordings and spectrograms from a sham (non-injected, WT) mouse (Ci) and from a mAGNET (virus-injected, WT) mouse (Cii) during 40 Hz pulse train laser illumination. Both LFP trace and spectrogram were aligned to illumination onset. Open boxes above indicate the time

(legend continued on next page)

regulating neural activity (Tan et al., 2013), and could potentially serve as biomarkers for brain diseases (Reed et al., 2018). Second, the small footprint of miRNA sites facilitates packaging into virus, an important mode of gene delivery to post-mitotic neurons. Finally, the combinatorial nature of miRNA regulation allows for the potential to engineer selectivity. For example, GABA mAGNETs could be designed to further specify targeting to subtypes of inhibitory neurons, such as parvalbumin, calretinin, or somatostatin neurons, by incorporating specific miRNA cassettes. mAGNETs are orthogonal to other gene regulatory strategies and thus can be easily combined with other cell targeting techniques. For example, short Dlx enhancer elements taken from the distal-less homeobox genes have been shown to be effective in targeting interneurons across several brain regions and species (Lee et al., 2014; Vogt et al., 2014; Dimidschstein et al., 2016). Incorporating the 400-bp-long mDlx enhancer in front of the short hSyn promoter in our AAV-GABA-mAGNET vector may further improve interneuron targeting selectivity in the rat brain.

Viral gene-targeting tools are especially valuable in murine disease models due to challenges in cross-breeding disease model animals with other transgenic cell-type-targeting lines. Our AAV co-delivery experiment demonstrates that AAV-GABA-mAGNET could be applied with other viral cell-type-labeling tools in a mouse model of autism to study the molecular mechanisms underlying excitation/inhibition (E/I) imbalance, a known feature of the disorder (Lee et al., 2017). In fact, this gene-targeting tool could be applied in a variety of murine transgenic disease models to study disease mechanisms (Marín 2012).

The mouse-derived GABA mAGNETs developed here also exhibited interneuron preference in the rat cortex (~74%–82% [Figure 3]) and hippocampus (~80% [Figure S3]). This suggests that miRNA-based targeting has potential in other animal models, including species where transgenic targeting is not possible or more difficult. Although genetic engineering techniques such as CRISPR are yielding promising results in rats (Li et al., 2013) and nonhuman primates (Sato and Sasaki 2018), transgenic targeting has historically been difficult in these species. While the GABA mAGNET was not as specific in the rat brain as in the mouse, it may provide a useful interim research tool. In the future, systematic analysis of cell-type- and brain-region-specific miRNA profiles in other species would greatly advance the design of mAGNETs for use in species where transgenic options are less readily available.

With advancements in genetically encoded neurotechnologies, a need has arisen for methods of genetically targeting independent neuron subtypes in the same animal. Here, we showed that mAGNETs can be used in conjunction with other promoter-based labeling techniques to optogenetically manipulate separate neuron subtypes in wild-type animals. This approach could also be implemented within transgenic animals (Reijmers et al., 2007) to further expand the number of cell types targeted. The results of our experiment stimulating excitatory neurons at 40 Hz are consistent with previous reports that periodic stimulation with blue laser light can activate and entrain ChR2-expressing neurons (Boyden et al., 2005) and LFP power at those frequencies (Iaccarino et al., 2016). Interestingly, we also found that periodic silencing of the inhibitory neurons could also entrain cortical rhythms, likely through disinhibition of the excitatory neurons and/or post-illumination rebound of inhibitory neurons (Chuong et al., 2014) or both. The observation that silencing inhibitory neurons produced less impact than activating excitatory neurons could potentially be due to the fact that inhibitory neurons only constitute a small fraction of the neural population (< 20%).

In the future, miRNA-based genetic classifiers could play a critical role in both basic neuroscience research and human gene therapy. Further cell-type-specific sequencing of miRNAs (Alberti et al., 2018) will allow the design of mAGNETs to target a greater repertoire of neuron types across more species. In addition to targeting known cell types, mAGNETs could also be useful for defining new neuron subtypes. The recent development of single-cell transcriptomics has shed light on the genetic diversity among neurons (Zeisel et al., 2015; Tasic, et al., 2016), suggesting that neuron identity may be too complex to be defined by the expression of one marker gene. Furthermore, mAGNETs may have significance for human gene therapy. Virus is currently the most promising method of therapeutic gene delivery in the central nervous system (Maguire et al., 2014), and the ability to virally target therapeutic transgenes to specific neuronal populations in the human brain would aid the development of better treatments for neurodegenerative and neuropsychiatric disorders. MicroRNAs are already being explored for knocking down gene therapies in off-target tissues (Geisler and Fechner 2016); thus. it's feasible that the mAGNET approach illustrated here for mice could be further developed to target neuron subtypes in the human brain. The GABA mAGNET presented here provides a means of virally labeling interneurons in the rodent brain and opens the door for the development of many more miRNA-based tools to advance neuroscience research and possibly human gene therapy.

EXPERIMENTAL PROCEDURES

Detailed descriptions are provided in the Supplemental Information. All procedures were in accordance with the NIH Guide for Laboratory Animals and approved by the Boston University Animal Care and Use and Biosafety Committees. Adult female wild-type C57BL/6J mice, FVP/NJ-Tg(Ube3a)1Mpan/J autism model mice, and adult male Sprague-Dawley wild-type rats were used. High-titer replication-incompetent lentivirus and AAVs were prepared and injected into the cortex and the hippocampus via custom hardware.

window for calculating oscillation power and solid parts indicate illumination duration: pre-illumination (Pre), red laser illumination (R), blue laser illumination (B), and simultaneous red and blue laser illumination (R+B).

(D) Normalized oscillation power during 40 Hz pulse train laser illumination across animals (sham: n = 5, mAGNET: n = 6).

(E) Gamma oscillations (30–50 Hz) induced by 40 Hz pulse train laser illumination with red laser (left), blue laser (middle), or both (right) in sham and mAGNET mice (*$p < 0.05$, Wilcoxon rank-sum test). Plot shows mean ± SEM.

(F–H) Same as (C–E), for 200 ms pulse laser illumination.

See also Table S2.

Optogenetic control experiments were performed when mice were awake and head-fixed. LFP recordings were made with a glass electrode, and laser illumination was delivered through optical fibers coupled with the glass electrode. Immunohistology was performed with antibodies against GABA, CamKIIα, followed by secondary antibodies and ToPRO-3 nuclear dye for visualization. Brain slices were imaged on an Olympus FV1000 scanning confocal microscope, and co-localization was quantified manually. Two statistical tests were used throughout this work. Interneuron targeting selectivity was assessed with a Pearson's chi-square test of independence with one degree of freedom (as cortical neurons examined are either excitatory or inhibitory). Optogenetic control-induced LFP power changes were assessed with a Wilcoxon rank-sum test.

DATA AND SOFTWARE AVAILABILITY

The accession numbers for the viral vector sequences reported in this paper are GenBank: (LV-GABA-mAGNET) MH458076, (LV-Control) MH458077, (AAV-GABA-mAGNET) MH458078, (AAV-Control) MH58079, (AAV-CamKIIalpha-mRuby2) MH58080, (AAV-Jaws-GABA-mAGNET) MH458081, (AAV-CamKIIalpha-ChR2) MH458082.

SUPPLEMENTAL INFORMATION

Supplemental Information includes Supplemental Experimental Procedures, three figures, and two tables and can be found with this article online at https://doi.org/10.1016/j.celrep.2018.06.049.

ACKNOWLEDGMENTS

X.H. acknowledges funding from NIH Director's New Innovator Award 1DP2NS082126, NINDS 1R01NS087950-01, Pew Foundation, Alfred P. Sloan Foundation, and Boston University Biomedical Engineering Department. M.K.K. acknowledges NIH F31NS095465-02. H.Y.M. acknowledges NIH R01MH079407. We thank Shamsh Shaikh and Kimberly Ching for helping to optimize immunohistology and confocal imaging. We thank Yuda Huo for providing instruction on producing AAV viruses and Zachary Gardner for breeding *Ube3a* (2xTg) autism mice.

AUTHOR CONTRIBUTIONS

M.K. and X.H. conceived of and designed all experiments and wrote the manuscript. M.K. performed all molecular cloning, virus preparation, and mouse surgeries and analyzed all confocal data. H.T. performed electrophysiology experiments, analyzed resulting data, and contributed to writing the manuscript. T.T. performed immunohistology and confocal imaging. H.G. performed rat surgeries and contributed to editing the manuscript. H.M. provided *Ube3a* (2xTg) and WT littermate mice and contributed to editing the manuscript.

DECLARATION OF INTERESTS

The authors declare no competing financial interests.

Received: February 8, 2018
Revised: April 3, 2018
Accepted: June 11, 2018
Published: July 10, 2018

REFERENCES

Alberti, C., Manzenreither, R.A., Sowemimo, I., Burkard, T.R., Wang, J., Mahofsky, K., Ameres, S.L., and Cochella, L. (2018). Cell-type specific sequencing of microRNAs from complex animal tissues. Nat. Methods *15*, 283–289.

Aschauer, D.F., Kreuz, S., and Rumpel, S. (2013). Analysis of transduction efficiency, tropism, and axonal transport of AAV serotypes 1, 2, 5, 6, 8 and 9 in the mouse brain. PLoS ONE *8*, e76310.

Bak, M., Silahtaroglu, A., Møller, M., Christensen, M., Rath, M.F., Skryabin, B., Tommerup, N., and Kauppinen, S. (2008). MicroRNA expression in the adult mouse central nervous system. RNA *14*, 432–444.

Blessing, D., and Déglon, N. (2016). Adeno-associated virus and lentivirus vectors: a refined toolkit for the central nervous system. Curr. Opin. Virol. *21*, 61–66.

Boyden, E.S., Zhang, F., Bamberg, E., Nagel, G., and Deisseroth, K. (2005). Millisecond-timescale, genetically targeted optical control of neural activity. Nat. Neurosci. *8*, 1263–1268.

Chuong, A.S., Miri, M.L., Busskamp, V., Matthews, G.A., Acker, L.C., Sørensen, A.T., Young, A., Klapoetke, N.C., Henninger, M.A., Kodandaramaiah, S.B., et al. (2014). Noninvasive optical inhibition with a red-shifted microbial rhodopsin. Nat. Neurosci. *17*, 1123–1129.

Delzor, A., Dufour, N., Petit, F., Guillermier, M., Houitte, D., Auregan, G., Brouillet, E., Hantraye, P., and Déglon, N. (2012). Restricted transgene expression in the brain with cell-type specific neuronal promoters. Hum. Gene Ther. Methods *23*, 242–254.

Dimidschstein, J., Chen, Q., Tremblay, R., Rogers, S.L., Saldi, G.A., Guo, L., Xu, Q., Liu, R., Lu, C., Chu, J., et al. (2016). A viral strategy for targeting and manipulating interneurons across vertebrate species. Nat. Neurosci. *19*, 1743–1749.

Dittgen, T., Nimmerjahn, A., Komai, S., Licznerski, P., Waters, J., Margrie, T.W., Helmchen, F., Denk, W., Brecht, M., and Osten, P. (2004). Lentivirus-based genetic manipulations of cortical neurons and their optical and electrophysiological monitoring in vivo. Proc. Natl. Acad. Sci. USA *101*, 18206–18211.

Geisler, A., and Fechner, H. (2016). MicroRNA-regulated viral vectors for gene therapy. World J. Exp. Med. *6*, 37–54.

Gonchar, Y., Wang, Q., and Burkhalter, A. (2008). Multiple distinct subtypes of GABAergic neurons in mouse visual cortex identified by triple immunostaining. Front. Neuroanat. *1*, 3.

Gray, S.J., Woodard, K.T., and Samulski, R.J. (2010). Viral vectors and delivery strategies for CNS gene therapy. Ther. Deliv. *1*, 517–534.

He, M., Liu, Y., Wang, X., Zhang, M.Q., Hannon, G.J., and Huang, Z.J. (2012). Cell-type-based analysis of microRNA profiles in the mouse brain. Neuron *73*, 35–48.

Iaccarino, H.F., Singer, A.C., Martorell, A.J., Rudenko, A., Gao, F., Gillingham, T.Z., Mathys, H., Seo, J., Kritskiy, O., Abdurrob, F., et al. (2016). Gamma frequency entrainment attenuates amyloid load and modifies microglia. Nature *540*, 230–235.

Klapoetke, N.C., Murata, Y., Kim, S.S., Pulver, S.R., Birdsey-Benson, A., Cho, Y.K., Morimoto, T.K., Chuong, A.S., Carpenter, E.J., Tian, Z., et al. (2014). Independent optical excitation of distinct neural populations. Nat. Methods *11*, 338–346.

Kügler, S., Kilic, E., and Bähr, M. (2003). Human synapsin 1 gene promoter confers highly neuron-specific long-term transgene expression from an adenoviral vector in the adult rat brain depending on the transduced area. Gene Ther. *10*, 337–347.

Lagos-Quintana, M., Rauhut, R., Yalcin, A., Meyer, J., Lendeckel, W., and Tuschl, T. (2002). Identification of tissue-specific microRNAs from mouse. Curr. Biol. *12*, 735–739.

Lee, A.T., Gee, S.M., Vogt, D., Patel, T., Rubenstein, J.L., and Sohal, V.S. (2014). Pyramidal neurons in prefrontal cortex receive subtype-specific forms of excitation and inhibition. Neuron *81*, 61–68.

Lee, E., Lee, J., and Kim, E. (2017). Excitation/Inhibition Imbalance in Animal Models of Autism Spectrum Disorders. Biol. Psychiatry *81*, 838–847.

Li, D., Qiu, Z., Shao, Y., Chen, Y., Guan, Y., Liu, M., Li, Y., Gao, N., Wang, L., Lu, X., et al. (2013). Heritable gene targeting in the mouse and rat using a CRISPR-Cas system. Nat. Biotechnol. *31*, 681–683.

Maguire, C.A., Ramirez, S.H., Merkel, S.F., Sena-Esteves, M., and Breakefield, X.O. (2014). Gene therapy for the nervous system: challenges and new strategies. Neurotherapeutics *11*, 817–839.

Marín, O. (2012). Interneuron dysfunction in psychiatric disorders. Nat. Rev. Neurosci. *13*, 107–120.

Minami, K., Uehara, T., Morikawa, Y., Omura, K., Kanki, M., Horinouchi, A., Ono, A., Yamada, H., Ohno, Y., and Urushidani, T. (2014). miRNA expression atlas in male rat. Sci. Data *1*, 140005.

Nathanson, J.L., Jappelli, R., Scheeff, E.D., Manning, G., Obata, K., Brenner, S., and Callaway, E.M. (2009a). Short Promoters in Viral Vectors Drive Selective Expression in Mammalian Inhibitory Neurons, but do not Restrict Activity to Specific Inhibitory Cell-Types. Front. Neural Circuits *3*, 19.

Nathanson, J.L., Yanagawa, Y., Obata, K., and Callaway, E.M. (2009b). Preferential labeling of inhibitory and excitatory cortical neurons by endogenous tropism of adeno-associated virus and lentivirus vectors. Neuroscience *161*, 441–450.

Nelson, S.B., and Valakh, V. (2015). Excitatory/Inhibitory Balance and Circuit Homeostasis in Autism Spectrum Disorders. Neuron *87*, 684–698.

Nelson, P.T., Wang, W.X., and Rajeev, B.W. (2008). MicroRNAs (miRNAs) in neurodegenerative diseases. Brain Pathol. *18*, 130–138.

Reed, E.R., Latourelle, J.C., Bockholt, J.H., Bregu, J., Smock, J., Paulsen, J.S., and Myers, R.H.; PREDICT-HD CSF ancillary study investigators (2018). MicroRNAs in CSF as prodromal biomarkers for Huntington disease in the PREDICT-HD study. Neurology *90*, e264–e272.

Reijmers, L.G., Perkins, B.L., Matsuo, N., and Mayford, M. (2007). Localization of a stable neural correlate of associative memory. Science *317*, 1230–1233.

Rudy, B., Fishell, G., Lee, S., and Hjerling-Leffler, J. (2011). Three groups of interneurons account for nearly 100% of neocortical GABAergic neurons. Dev. Neurobiol. *71*, 45–61.

Santhekadur, P.K., Das, S.K., Gredler, R., Chen, D., Srivastava, J., Robertson, C., Baldwin, A.S., Jr., Fisher, P.B., and Sarkar, D. (2012). Multifunction protein staphylococcal nuclease domain containing 1 (SND1) promotes tumor angiogenesis in human hepatocellular carcinoma through novel pathway that involves nuclear factor κB and miR-221. J. Biol. Chem. *287*, 13952–13958.

Sato, K., and Sasaki, E. (2018). Genetic engineering in nonhuman primates for human disease modeling. J. Hum. Genet. *63*, 125–131.

Sayeg, M.K., Weinberg, B.H., Cha, S.S., Goodloe, M., Wong, W.W., and Han, X. (2015). Rationally Designed MicroRNA-Based Genetic Classifiers Target Specific Neurons in the Brain. ACS Synth. Biol. *4*, 788–795.

Smith, S.E., Zhou, Y.D., Zhang, G., Jin, Z., Stoppel, D.C., and Anderson, M.P. (2011). Increased gene dosage of Ube3a results in autism traits and decreased glutamate synaptic transmission in mice. Sci. Transl. Med. *3*, 103ra97.

Tamamaki, N., Yanagawa, Y., Tomioka, R., Miyazaki, J., Obata, K., and Kaneko, T. (2003). Green fluorescent protein expression and colocalization with calretinin, parvalbumin, and somatostatin in the GAD67-GFP knock-in mouse. J. Comp. Neurol. *467*, 60–79.

Tan, C.L., Plotkin, J.L., Venø, M.T., von Schimmelmann, M., Feinberg, P., Mann, S., Handler, A., Kjems, J., Surmeier, D.J., O'Carroll, D., et al. (2013). MicroRNA-128 governs neuronal excitability and motor behavior in mice. Science *342*, 1254–1258.

Taniguchi, H., He, M., Wu, P., Kim, S., Paik, R., Sugino, K., Kvitsiani, D., Fu, Y., Lu, J., Lin, Y., et al. (2011). A resource of Cre driver lines for genetic targeting of GABAergic neurons in cerebral cortex. Neuron *71*, 995–1013.

Tasic, B., Menon, V., Nguyen, T.N., Kim, T.K., Jarsky, T., Yao, Z., Levi, B., Gray, L.T., Sorensen, S.A., Dolbeare, T., et al. (2016). Adult mouse cortical cell taxonomy revealed by single cell transcriptomics. Nat. Neurosci. *19*, 335–346.

Tremblay, R., Lee, S., and Rudy, B. (2016). GABAergic Interneurons in the Neocortex: From Cellular Properties to Circuits. Neuron *91*, 260–292.

Vogt, D., Hunt, R.F., Mandal, S., Sandberg, M., Silberberg, S.N., Nagasawa, T., Yang, Z., Baraban, S.C., and Rubenstein, J.L. (2014). Lhx6 directly regulates Arx and CXCR7 to determine cortical interneuron fate and laminar position. Neuron *82*, 350–364.

Watakabe, A., Ohtsuka, M., Kinoshita, M., Takaji, M., Isa, K., Mizukami, H., Ozawa, K., Isa, T., and Yamamori, T. (2015). Comparative analyses of adeno-associated viral vector serotypes 1, 2, 5, 8 and 9 in marmoset, mouse, and macaque cerebral cortex. Neurosci. Res. *93*, 144–157.

Xu, R., Janson, C.G., Mastakov, M., Lawlor, P., Young, D., Mouravlev, A., Fitzsimons, H., Choi, K.L., Ma, H., Dragunow, M., et al. (2001). Quantitative comparison of expression with adeno-associated virus (AAV-2) brain-specific gene cassettes. Gene Ther. *8*, 1323–1332.

Xu, X., Roby, K.D., and Callaway, E.M. (2006). Mouse cortical inhibitory neuron type that coexpresses somatostatin and calretinin. J. Comp. Neurol. *499*, 144–160.

Zeisel, A., Muñoz-Manchado, A.B., Codeluppi, S., Lönnerberg, P., La Manno, G., Juréus, A., Marques, S., Munguba, H., He, L., Betsholtz, C., et al. (2015). Brain structure. Cell types in the mouse cortex and hippocampus revealed by single-cell RNA-seq. Science *347*, 1138–1142.

Cell Reports, Volume *24*

Supplemental Information

A MicroRNA-Based Gene-Targeting Tool for Virally Labeling Interneurons in the Rodent Cortex

Marianna K. Keaveney, Hua-an Tseng, Tina L. Ta, Howard J. Gritton, Heng-Ye Man, and Xue Han

Supplemental Tables and Figures

SUMMARY OF INTERNEURON LABELLING			
Virus Type	Animal and Injection site	GABA Colocalization[e,f]	
		mAGNET	Control
LV	C57BL/6 wt mouse[a] (cortex 1 & 2)[d]	91 ± 3% *** (339)	12 ± 3% (384)
	Sprague-Dawley wt rat[a] (cortex 1 & 2) [d]	74 ± 3% *** (337)	16 ± 3% (408)
AAV	C57BL/6 wt mouse[a] (cortex 1)	98 ± 2% *** (184)	23 ± 2% (195)
	FVP/NJ-Tg(Ube3a)1Mpan/J mouse[b] (cortex 1)	96 ± 2% (134)	NA
	FVB/NJ wt mouse[c] (cortex 1)	95 ± 3% (177)	NA
	Sprague-Dawley wt rat[a] (cortex 1 & 2) [d]	82 ± 3% *** (348)	21 ± 4% (411)
	Sprague-Dawley wt rat[a] (hippocampus)	80 ± 5% *** (176)	8 ± 2% (174)

Table S1. Summary of interneuron labelling. Related to Figures 1, 2 and 3.

[a] n = 3 animals each for GABA mAGNET and Control virus
[b] n = 2 animals, GABA mAGNET virus only
[c] n = 3 animals, GABA mAGNET virus only
[d] data are pooled across both cortical injection sites
[e] numbers in parentheses indicate the number of EGFP+ neurons analyzed (at least 50 per animal per injection site, see Methods)
[f] *** $p<0.005$ Pearson's chi squared test (see Supplemental Experimental Procedures).

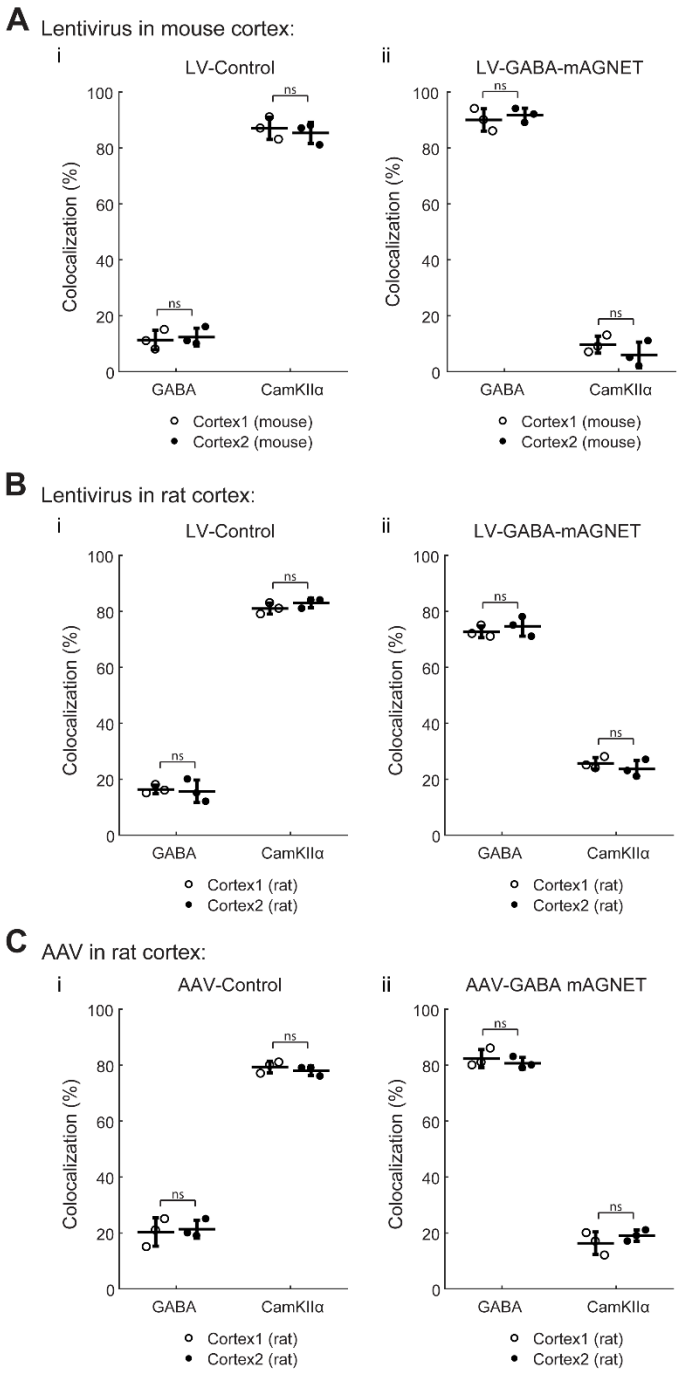

Figure S1. Consistency in interneuron targeting across cortical injection sites. Related to Figures 1, 2 and 3. (A) – (C) Comparison of EGFP colocalization (%) with immunohistology markers for inhibitory neurons (GABA) or excitatory neurons (CamKIIα) - reveals no significant differences (ns, Pearson's chi squared test) between the two motor cortex sites injected for (A) lentiviruses in the mouse cortex, (B) lentiviruses in the rat cortex, or (C) AAVs in the rat cortex. Note that AAVs were only injected at one site in the mouse cortex, so there is no comparison data across cortical sites. Scatter plots show individual animals (circles) and mean (horizontal bar) ± SD.

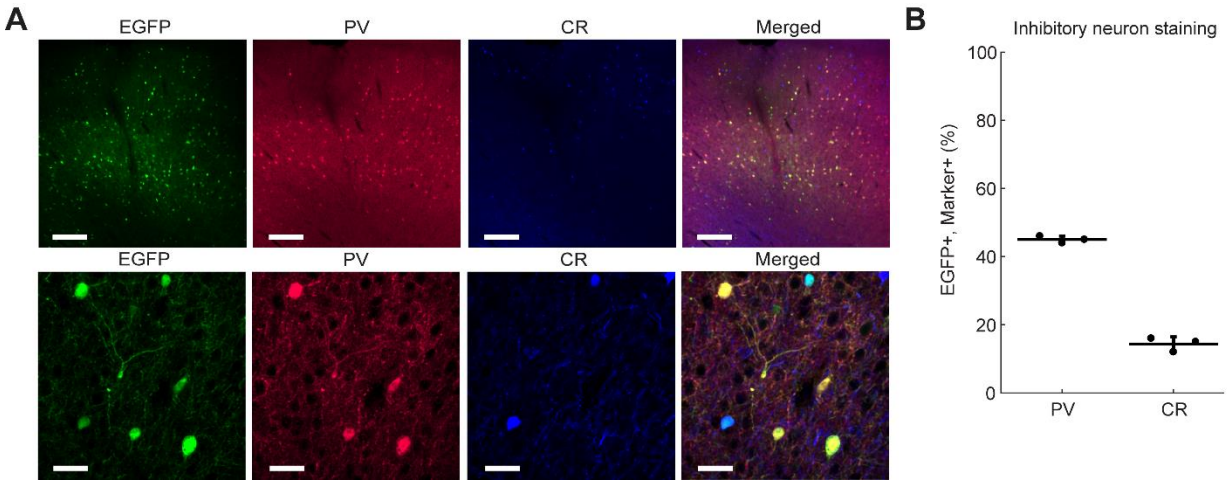

Figure S2. AAV-GABA-mAGNET labelling of interneuron subtypes by cortical layer. Related to Figure 2.
(A) Representative confocal images of EGFP fluorescence from cortical cells transduced with AAV GABA mAGNET, immunofluorescence of non-overlapping parvalbumin (PV) and calretinin (CR) cell markers, and colocalization at low (top) and high (bottom) magnification. Top scale bars are 210 µm. Bottom scale bars are 35 µm.
(B) Colocalization of EGFP (%) with PV and CR marker immune stains in the wild type mouse cortex (n = 3 mice). Scatter plot shows individual animals (circles) and mean (horizontal bar) ± SD. Colocalization of EGFP (%) with immunohistology markers for sub-types of inhibitory neurons – parvalbumin (PV) and calretinin (CR) – follows the expected distribution of these cells in mouse cortex.

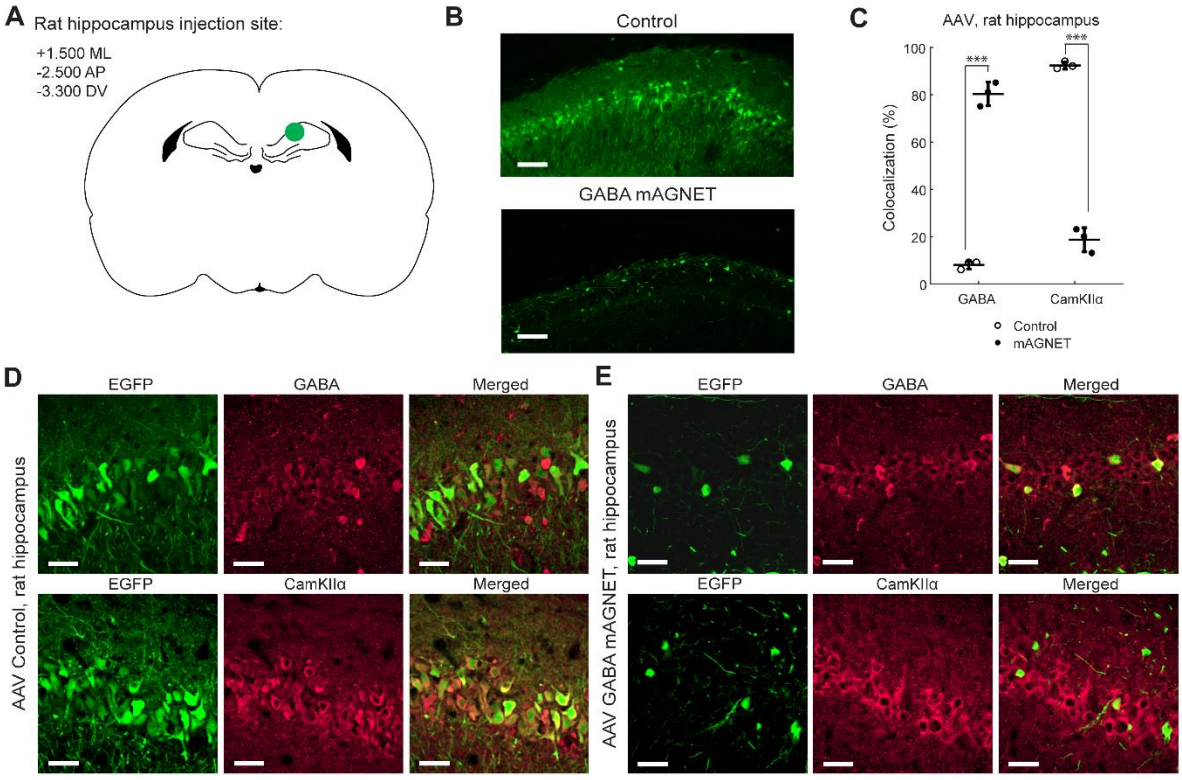

Figure S3. AAV-GABA-mAGNET targeting in the wild type rat hippocampus. Related to Figure 3.

(A) Schematic of stereotaxic virus injection sites in rat hippocampus.

(B) Confocal microscopy images showing comparison of AAV-Control and AAV-mAGNET-transduction in rat hippocampus. Scale bars are 250 µm.

(C) Colocalization of EGFP with inhibitory (GABA) and excitatory (CamKIIα) neuron marker immune stains in the rat hippocampus (n = 3 rats each). Scatter plot shows individual animals (circles) and mean (horizontal bar) ± SD. ***: $p<0.005$ Pearson's chi squared test (see Methods).

(D) Representative confocal images of EGFP fluorescence from cortical cells transduced with AAV-Control, immunofluorescence of inhibitory (GABA) and excitatory (CamKIIα) cell markers, and colocalization. Scale bars are 35 µm.

(E) Same as (D), for cells transduced with AAV-GABA-mAGNET.

Supplemental Experimental Procedures

Viral vector construction. Standard molecular cloning procedures (PCR and restriction enzyme digestion) were used to construct genetic classifiers in viral vectors unless otherwise stated. LV GABA mAGNET and LV Control vectors were made by replacing the 1.2 kb Ef-1α promoter in our previously published 8X2C mAGNET (Addgene plasmid #67955) with human Synapsin 1 promoter (Addgene plasmid #86537) via EcoRI and BamHI restriction sites. The expression cassettes (including promoter, transgene and miRNA sites for mAGNET) from the resulting LV GABA mAGNET and LV Control vectors were amplified via PCR and inserted between the ITRs of an AAV-2 genomic vector obtained from Roger Tsien (Addgene plasmid #50954) via BglII and HindIII restriction sites. To produce the AAV CamKIIα mRuby2 vector, the CamKIIα promoter obtained from Ed Boyden (Addgene plasmid #64545) was cloned into the AAV-2 vector simultaneously with an mRuby2 reporter obtained from Michael Davidson (Addgene plasmid #54771) via EcoRI, AscI and Sbf1 sites. To generate Jaws GABA mAGNET, the Jaws transgene fused to an ER2 tag was obtained from Ed Boyden (Addgene plasmid #65013) and fused to mRuby2, replacing EGFP in the AAV GABA mAGNET and AAV Control vectors via a Gibson reaction. Finally, the CamKIIα ChR2 vector was produced by replacing the mRuby2 transgene in the AAV CamKIIα mRuby2 vector with ChR2-EGFP obtained from Ed Boyden (Addgene plasmid #58881) via AscI and SpeI sites. For sequences, see Supplementary Table 1. All new viral vectors produced here will be deposited to GenBank and Addgene.

Lentivirus preparation. Replication-incompetent lentivirus was packaged via triple transfections of the LV-hSyn-EGFP or LV-hSyn-EGFP-8X2C lentiviral transfer plasmid, plasmid pMD2.G encoding for VSV-G pseudotyping coat protein (Addgene plasmid #12259), and pDelta 8.74 (Addgene plasmid #5682) helper packaging plasmid, into HEK293FT cells (LifeTechnologies, R700-07) using TransIT-293 transfection reagent (Mirus Bio LLC, MIR 2700),

and then purified through ultracentrifugation. Viral transduction was first tested in primary rat neuron cultures before *in vivo* injections were performed, and viral titer was estimated to be ~1E9 transducing units/mL based on transduction efficiency of serial dilutions (Han, Qian et al. 2009).

Adeno-associated virus (AAV) preparation. Replication-incompetent AAV was packaged via triple transfections of the AAV-2 transfer vector (rAAV2.9-hSyn-EGFP-8XC, rAAV2.9-hSyn-EGFP, rAAV2.9-CamKIIα-mRuby2, rAAV2.9-hSyn-Jaws_mRuby2-8X2C, or rAAV2.9-CamKIIα-ChR2_EGFP), cap-9 plasmid encoding the Rep and Cap proteins (serotype 9), and pXX680 helper packaging plasmid, into HEK293FT cells (LifeTechnologies, R700-07) using TransIT-293 transfection reagent (Mirus Bio LLC, MIR 2700). Two days post-transfection, HEK cells were washed and lysed via three freeze-thaw cycles followed by sonication, and virus was purified from the lysate via PEG precipitation (System Biosciences, LV810A-1). Viral titer was determined via rt-PCR (Takara, AAVpro Titration Kit Ver.2) to be ~2E12 vg/mL. Viral transduction was first tested in primary rat neuron cultures before *in vivo* injections were performed.

Stereotaxic virus injection surgeries. All procedures were done in accordance with the National Institutes of Health Guide for Laboratory Animals and were approved by the Boston University Institutional Animal Care and Use and Biosafety Committees. Mice used for Figure 1, and 2A-E were adult female C57bL/6 wild type mice (Taconic Biosciences) eight weeks old at time of injection. We injected lentivirus at two locations in the mouse neocortex: cortex1 (+1.000 mm ML, +1.800 mm AP, -1.250 mm DV) and cortex2 (+1.000 mm ML, -1.500 mm AP, -0.900 mm DV). Approximately 1.0 µL (1E6 infectious particles) of lentivirus was injected per site. Three mice were injected per condition (n = 6 mice total). We injected the AAV GABA mAGNET or AAV Control only at the cortex 1 coordinates in the mouse cortex. Approximately 0.5 µL of virus was injected for each AAV (1E9 viral particles). Three mice were used per virus (n = 6 mice total).

Mice used in Figure 2F-I were adult female FVP/NJ-Tg(Ube3a)1Mpan/J autism mice (The Jackson Laboratory stock #019730) or adult female FVP/NJ wild type littermates (The Jackson Laboratory stock #001800), twelve weeks old at time of injection. To obtain Ube3a 2X Tg animals, heterozygous (1X Tg) males were mated with heterozygous (1X Tg) females, and the offspring homozygous (2X Tg) animals were used for experiments. We injected ~1.0 µL of AAV GABA mAGNET premixed with AAV CamKIIα mRuby2 (1E9 viral particles per virus) at the cortex 1 coordinates. Two Ube3a 2X Tg autism mice and three wild type littermates were used (n = 5 mice total).

All rats used were adult male Sprague-Dawley wild type rats, eight weeks old at the time of injection. We injected lentivirus at two locations in the rat brain: cortex 1 (+1.700 mm ML, +2.800 mm AP, -1.600 mm DV) and cortex 2 (+1.500 mm ML, -2.500 mm AP, -1.600 mm DV), analogous to the corresponding cortical injection sites in the mice. ~1.0 µL of lentivirus was injected per site. Three rats were injected per lentivirus (n = 6 rats total). ~0.5 µL AAV GABA mAGNET or AAV Control was injected at both cortical sites in the rats and additionally at a site in the hippocampus (+1.500 mm ML, -2.500 mm AP, -3.300 mm DV). Three rats each were used for each AAV virus (n = 6 rats total). All injection surgeries were performed using sterile surgical techniques under isoflurane anesthesia, and were accomplished using a standard rodent stereotaxic instrument and an automated microinjection syringe pump (World Precision Instruments, UMP3-1).

Immunohistology. At two weeks (LV) or three weeks (AAV) post-injection, animals were sacrificed and perfused with 4% PFA. Brains were post-fixed in 4% PFA for three hours, cryoprotected in a 30% sucrose, then flash froze in OCT. Frozen brains were sectioned (coronal) at 50 µm on a cryostat and slices were stored in PBS+0.05% sodium azide. Brian slices were stained with antibodies against GABA (Sigma, A2052, 1:1000) or CamKIIα (Santa Cruz Biotech, sc-13082, 1:50), followed by Alexa Fluor 568 goat anti-rabbit secondary antibody (Invitrogen A21071, 1:1000) and ToPRO-3 nuclear dye (Life Technologies, 1:5000), or just Alexa Fluor 633

goat anti-rabbit secondary antibody (Invitrogen A11011, 1:1000). The same GABA and CamKIIα primary antibodies (as well as Alexa Fluor secondary antibodies) were used for mice and rat brain slices, as they were shown by the manufacturer to be reactive in both species. For parvalbumin (PV) and calretinin (CR) staining, brain slices were co-stained with a mix of PV (SWANT GP72 1:2000) and CR antibodies (SWANT 7697 1:1000), and then a mix of secondary antibodies: Alexa Fluor 568 goat anti-guinea pig (Invitrogen A11075 1:1000) and Alexa Fluor 633 goat anti-rabbit secondary antibody (Invitrogen A11011, 1:1000).

Confocal imaging and quantification. Confocal imaging was performed on an Olympus FV1000 scanning confocal microscope, using a 10X lens or 60X water immersion lens. Z-stacks were taken by imaging at 2 µm intervals throughout the slices. Confocal image stacks were taken at least 150 µm away from the center of the injection site for LV, and at least 250 µm away from the center of the injection site for AAV. Consistent laser settings were used for all imaging sessions: 488 nm laser 3.5%, 350 V; 543 nm laser 13%, 600 V; 633 nm laser 5%, 600V. EGFP+ cell bodies were identified by comparison with ToPRO-3 nuclear staining, then each identified EGFP+ cell was categorized as immunopositive or immunonegative for the antibody stain. Note that staining for each immune marker (ex. GABA, CamKIIα) was performed on separate cortical brain slices unless otherwise stated. Immunopositive cell counts were pooled across slices stained for the same marker for each animal, and normalized to the total EGFP+ cell count across those slices. In this way, the proportion (%) of EGFP+ (or labelled) cells that colocalize with each immunomarker was calculated independently. Conversely, we determined that the cortical interneuron transduction efficiency of our AAVs at the delivered dose was 70 ± 3% (n = 246 cells), based on the percentage of GABA+ cells expressing the reporter, consistent with the general observation of the overall transduction efficiency of AAVs. For each animal, we analyzed at least 1-4 non-overlapping confocal stacks from each of 2-6 slices per injection site. A similar number of cells (at least 50 EGFP+ cells per animal, see Statistical analysis) at similar distances from the

injection site (~150 – 250 µm for LV and ~250 – 350 µm for AAV) were analyzed for each animal. All hippocampal images were taken in the CA1 area.

Statistical analysis. To determine the minimal sample size (number of animals) needed to ensure adequate power to detect an inhibitory neuron targeting effect, we performed a power analysis with the following parameters: mean control group estimated value = 0.2, mean experimental group estimated value = 0.8, expected standard deviation = 0.05, alpha = 0.05, power = 0.8, 2 sided test. Randomization and investigator blinding were not considerations of this study design.

A chi squared test of independence with one degree of freedom (as cortical neurons examined are either excitatory or inhibitory) requires an expected frequency of at least 10 to produce reliable approximations, and because inhibitory cells make up approximately 20% of neurons in the cortex, 50 neurons per mouse in each test condition was determined to be the minimum sample size. The Pearson's chi squared test statistic with one degree of freedom was calculated for interneuron targeting in each condition by taking the difference between the observed number of counts for inhibitory cells compared to the expected distribution of 20% inhibitory cells, to determine the statistical significance of the targeting effect.

Optogenetics and electrophysiology. All mice used were adult female C57bL/6 wild type mice. At eight weeks old, mAGNET mice (n = 6) were injected with ~1.0 µL an equal mixture (1E9 viral particles each) of AAV Jaws GABA mAGNET and AAV CamKIIα ChR2 at cortex 1 coordinates (+1.000 mm ML, +1.800 mm AP, -1.250 mm DV). During the same surgery, a metal pin was implanted in the opposite hemisphere serving as recording ground, and a head plate was secured to the animal's skull via dental cement. Sham animals (n = 5) underwent surgery for metal ground pin and head plate implantation, but did not receive any viral injection.

After 6-7 weeks post-surgery, recordings were performed with a borosilicate glass electrode (G100F-4, Warner Instruments; 1-5 MOhm and filled with saline) to avoid laser light induced artifact on metal electrodes, while mice were awake and head-fixed. Signals were amplified with a Multiclamp 700B (Molecular Device), digitized with a Digidata 1440A, and recorded with the pClamp software (Molecular Device) at 20 kHz. Optogenetic light illumination for ChR2 and Jaws were achieved with a 473 nm blue laser (Shanghai Laser) and a 635 nm red laser (Shanghai Laser), respectively. To deliver light, two optical fibers (200 μm in diameter, ThorLabs) were coupled with the glass electrode. The tips of the optical fibers were positioned about 500 μm above the tip of the glass electrode, and the power at the optic fiber tips was adjusted to 10 mW for both blue and red light. The fiber-electrode bundle was insert into the viral injection site (+1.000 mm ML, +1.800 mm AP, -0.400 DV). Illumination patterns consisted of three conditions: red laser alone to silence inhibitory neurons (R), blue laser alone to activate excitatory neurons (B), and both lasers (R+B). For each condition, we tested two illumination patterns (40 Hz pulse with 50% duty cycle, or a single constant pulse of 200 ms in duration). The illumination patterns were generated by a function generator (33210A Agilent), which was triggered by pClamp to maintain precise timing of the illumination patterns. Each trial contained three illumination periods (red laser alone, blue laser alone, and red + blue lasers) with 10 seconds intervals between each illumination and 5 second window before the first illumination period and after the last illumination period. The illumination order was randomized across mice, and each mouse underwent 10 trials of each illumination pattern.

Electrophysiology data analysis. LFP data analysis was performed in Matlab with Chronux (http://chronux.org/). Spectrograms were generated with mtspecgramc (tappers=[3 5], window size=500 ms, step size=5 ms) and normalized as decibel (dB) using: $power_{normalized} = 10 \times \log \frac{power}{power_{max}}$

where $power_{max}$ is the maximum value of the LFP power during each trial. The power pre- and post-stimulation for each trial was calculated with mtspectrumc (tappers=[3 5]) from LFP signals during the 1- second windows before and after illumination onset, respectively. To remove the variabilities between individuals, we further normalize the power for each illumination as follows:

$$power_{normalized} = 10 \times \log \frac{power}{power_{baseline}}$$

where $power_{baseline}$ is the averaged power during the 1-second window prior to the pre-illumination window. The powers were first averaged across trials to obtain the representative power for each animal, and then averaged across animals.